Inflation in a two 3-form fields scenario

[1,2]K. Sravan Kumar*, [1,2]João Marto†,
[3]Nelson J. Nunes‡, [1,2]Paulo Vargas Moniz§

4th July 2014

[1]Departamento de Física, Universidade da Beira Interior, 6200 Covilhã, Portugal.

[2]Centro de Matemática e Aplicações da Universidade da Beira Interior (CMA-UBI).

[3]Faculty of Sciences and Centre for Astronomy and Astrophysics, University of Lisbon, 1749-016 Lisbon, Portugal.

arXiv:1404.0211v2 [gr-qc] 3 Jul 2014

Abstract

A setting constituted by $\mathbb{N}$ 3-form fields, without any direct interaction between them, minimally coupled to gravity, is introduced in this paper as a framework to study the early evolution of the universe. We focus particularly on the two 3-forms case. An inflationary scenario is found, emerging from the coupling to gravity. More concretely, the fields coupled in this manner exhibit a complex interaction, mediated by the time derivative of the Hubble parameter. Our investigation is supported by means of a suitable choice of potentials, employing numerical methods and analytical approximations. In more detail, the oscillations on the small field limit become correlated, and one field is intertwined with the other. In this type of solution, a varying sound speed is present, together with the generation of isocurvature perturbations. The mentioned features allow to consider an interesting model, to test against observation. It is subsequently shown how our results are consistent with current CMB data (viz.Planck and BICEP2).

1 Introduction

The recent cosmic microwave background (CMB) studies, developed in the context of the Planck mission [1, 2, 3, 4], have brought important constraints into the domain of viable inflationary scenarios. In particular, these accurate measurements seem to favor simple inflationary slow roll models. They confirm with high accuracy that the universe is almost spatially flat; the fluctuations are nearly Gaussian, adiabatic, and showing a nearly scale invariant power spectrum. The observations also give strong support for a ΛCDM Universe. An inflationary period driven by a single scalar field has been the most widely studied approach in the literature. Nevertheless, our lack of a precise knowledge regarding the connection between the early universe and the standard model of particle physics allow us to consider models of inflation driven by multiple fields [5]. Moreover, recent advances in experimental particle physics, such as the evidence towards the discovery of the Higgs boson at a much lower mass scale than expected, motivate the study of multiple inflaton field scenarios. Such attempts have been considered in the past and the literature contains several examples, namely hybrid inflation [6], assisted inflation [7, 8] and k-inflation [9, 10] models. In the context of the string compactification we may also refer the multiple axion and assisted chaotic models [11, 12]. Therefore, it is important to test inflationary models against Planck data.

Besides scalar field models, inflation driven by higher spinor fields has also been investigated. These models have a crucial importance due to the possible connection to string compactification scenarios[13, 14]. Among these approaches, we mention inflation obtained by means of vector fields [15, 16, 17]. Other important examples are p-form inflationary models [18, 19]. Therein, the scalar and vector fields constitute[1] the 0-form and 1-form cases in the wider classification of p-forms. A most relevant feature of non minimal interactions of massive p-forms with gravity is that it clearly supports an inflationary background

*sravan@ubi.pt
†jmarto@ubi.pt
‡njnunes@fc.ul.pt
§pmoniz@ubi.pt

[1]It is shown that higher p-form fields can ultimately be dualized to 0 and 1-forms.

[19, 20]. However, it has been shown that 1-form and 2-form are plagued by a ghost instability during inflation and are also unable to provide a satisfactory explanation of the CMB isotropy. Nevertheless, 0-form and 3-form fields are compatible with homogeneity and isotropy. Ref. [20] includes a study about p-form inflation. It is concluded that 3-form field inflation is similar to the one driven with a scalar field and that it is free from negative values for the squared propagation speed of the gravitational waves (which are characteristic of large field 2-form models). Considered as a suitable alternative to the traditional scalar field inflation, single 3-form inflation has been introduced and studied in Ref. [21, 22, 23]. In [23] a suitable choice of the potential for the 3-form has been proposed in order to avoid ghosts and Laplacian instabilities; the authors have shown that potentials showing a quadratic dominance, in the small field limit, would introduce sufficient oscillations for reheating [24] and would be free of ghost instabilities.

In this work, we extend the single 3-form framework to $\mathbb{N}$ 3-forms, to investigate in particular the early universe driven by two 3-forms. Being more precise, in section 2 we identify basic features of $\mathbb{N}$ 3-forms slow roll solutions, which can be classified into two types. We also discuss how the inflaton mass can be brought to lower energy scales, for large values of $\mathbb{N}$. In section 3 we examine the possible inflationary solutions, when two 3-forms are present. There are two classes, namely solutions not able to generate isocurvature perturbations (type I); and solutions with inducing isocurvature effects (type II). Our major objective is to understand and explore the cosmological consequences of type II solutions. More concretely, we will show that type II brings about interesting effects. In particular, we use a dynamical system analysis and conclude that type I case is very similar to single 3-form inflation [23, 22]. Type II case, however, characterizes a new behavior, through curved trajectories in field space. Moreover, type II inflation is clearly dominated by the gravity mediated coupling term which appears in the equations of motion. We present and discuss type II solutions for several classes of potentials, which are free from ghost instabilities [23] and show evidence of a satisfactory oscillatory behavior at the end of the two 3-forms driven inflation period. We also provide analytical arguments to explain the oscillatory behavior present in this choice of potentials. In addition, we calculate the speed of sound, c_s^2, of adiabatic perturbations for two 3-forms and show it has significant variations during inflation for type II solutions. In section 4 we discussed adiabatic and entropy perturbations for two 3-form fields, using a dualized action [25, 26]. We distinguish, type I and type II solutions with respect to isocurvature perturbations and calculate the power spectrum expression [27]. In section 5 we present how our inflationary setting can fit the tensor scalar ratio, spectral index and its running provided by the Planck data as well as the recent BICEP2 results [1, 28]. In section 6 we summarize and discuss the model herein investigated and propose subsequent lines to explore. Appendix A provides stability analysis regarding type I solutions.

2 $\mathbb{N}$ 3-form fields model

In this section, we generalize the background equations associated to a single 3-form field, which has been studied in [21, 22, 23], to $\mathbb{N}$ 3-form fields. We take a flat Friedmann-Lemaitre-Robertson-Walker (FLRW) cosmology, described with the metric

$$ds^2 = -dt^2 + a^2(t)d\boldsymbol{x}^2, \tag{2.1}$$

where $a(t)$ is the scale factor with t being the cosmic time. The general action for Einstein gravity and $\mathbb{N}$ 3-form fields is written as

$$S = -\int d^4x\sqrt{-g}\left[\frac{1}{2\kappa^2}R - \sum_{n=1}^{\mathbb{N}}\left(\frac{1}{48}F_n^2 + V_n(A_n^2)\right)\right], \quad \kappa^2 = 8\pi G\,, \tag{2.2}$$

where $A^{(n)}_{\beta\gamma\delta}$ is the nth 3-form field and we have squared the quantities by contracting all the indices. The strength tensor of the 3-form is given by[2]

$$F^{(n)}_{\alpha\beta\gamma\delta} \equiv 4\nabla_{[\alpha}A^{(n)}_{\beta\gamma\delta]}, \tag{2.3}$$

where antisymmetrization is denoted by square brackets. As we have assumed a homogeneous and isotropic universe, the 3-form fields depend only on time and hence only the space like components will be dynamical, thus their nonzero components are given by

$$A^{(n)}_{ijk} = a^3(t)\epsilon_{ijk}\chi_n(t) \quad \Rightarrow A_n^2 = 6\chi_n^2, \tag{2.4}$$

[2]Throughout this paper, the Latin index n will be used to refer the number of the quantity (or the 3-form field) or the nth quantity/field. The other Latin indices, which take the values $i, j = 1, 2, 3$, will indicate the three dimensional quantities; whereas the Greek indices will be used to denote four-dimensional quantities and they stand for $\mu, \nu = 0, 1, 2, 3$.

where $\chi_n(t)$ is a comoving field associated to the nth 3-form field and ϵ_{ijk} is the standard three dimensional Levi-Civita symbol. Also note that by introducing the more convenient field $\chi_n(t)$, which is related to the corresponding 3-form field by the above relation, we have, subsequently, the following system of equations of motion for $\mathbb{N}$ 3-form fields

$$\ddot{\chi}_n + 3H\dot{\chi}_n + 3\dot{H}\chi_n + V_{(n),\chi_n} \quad = 0, \tag{2.5}$$

where $V_{(n)} \equiv V_n(\chi_n)$ and $V_{(n),\chi_n} \equiv \frac{dV_{(n)}}{d\chi_n}$. For each value of n , each of the Eqs. (2.5) are not independent: it is straightforward to see that a peculiar coupling is present through the Hubble parameter derivative, $\dot{H}$. This fact will play a crucial role, establishing different classes of inflationary behavior when more than one three-from field is employed. In this setting, the gravitational sector equations are given by

$$H^2 = \frac{\kappa^2}{3}\left\{\frac{1}{2}\sum_{n=1}^{\mathbb{N}}\left[\left(\dot{\chi}_n + 3H\chi_n\right)^2 + 2V_{(n)}\right]\right\}, \tag{2.6}$$

$$\dot{H} = -\frac{\kappa^2}{2}\left[\sum_{n=1}^{\mathbb{N}} V_{(n),\chi_n}\chi_n\right]. \tag{2.7}$$

Therefore, the mentioned (gravity mediated) coupling between the several $\mathbb{N}$ 3-form fields will act through the gravitational sector of the equations of motion. The total energy density and pressure of the $\mathbb{N}$ 3-form fields read

$$\rho_{\mathbb{N}} = \frac{1}{2}\sum_{n=1}^{\mathbb{N}}\left[\left(\dot{\chi}_n + 3H\chi_n\right)^2 + 2V_{(n)}\right], \tag{2.8}$$

$$p_{\mathbb{N}} = -\frac{1}{2}\sum_{n=1}^{\mathbb{N}}\left[\left(\dot{\chi}_n + 3H\chi_n\right)^2 + 2V_{(n)} - 2V_{(n),\chi_n}\chi_n\right]. \tag{2.9}$$

We rewrite Eq. (2.5) as

$$\ddot{\chi}_n + 3H\dot{\chi}_n + V^{\text{eff}}_{n,\chi_n} \quad = 0,, \tag{2.10}$$

where

$$V^{\text{eff}}_{n,\chi_n} \equiv 3\dot{H}\chi_n + V_{(n),\chi_n} = V_{(n),\chi_n}\left[1 - \frac{3\kappa^2}{2}\chi_n^2\right] - \frac{3}{2}\kappa^2\chi_n\left[\sum_{\substack{m=1\\ n\neq m}}^{\mathbb{N}} V_{(m),\chi_m}\chi_m\right]. \tag{2.11}$$

In order to describe the dynamics of the 3-form fields, we express the equations of motion in terms of the dimensionless variables,

$$\begin{aligned} x_n &\equiv \kappa\,\chi_n, \\ w_n &\equiv \frac{\chi_n' + 3\chi_n}{\sqrt{6}}, \end{aligned} \tag{2.12}$$

where $x_n' \equiv dx_n/dN$ in which the number of e-folds of inflationary expansion is $N = \ln a(t)$. Thus, we get

$$H^2 x_n'' + \left(3H^2 + \dot{H}\right)x_n' + V^{\text{eff}}_{n,x_n} \quad = \quad 0. \tag{2.13}$$

The Friedmann constraint is written as

$$H^2 = \frac{1}{3}\frac{\sum_{n=1}^{\mathbb{N}} V_{(n)}}{(1-w^2)}, \tag{2.14}$$

where

$$w^2 \equiv \sum_{n=1}^{\mathbb{N}} w_n^2.$$

Employing the dimensionless variables (2.12), the equations of motion (2.13) can be rewritten in the autonomous form as

$$x_n' = 3\left(\sqrt{\frac{2}{3}}w_n - x_n\right), \tag{2.15}$$

$$w_n' = \frac{3}{2}\frac{V_{(n),x_n}}{V}\left(1-w^2\right)\left(x_n w_n - \sqrt{\frac{2}{3}}\right) + \frac{3}{2}\left(1-w^2\right)\frac{1}{V}w_n\sum_{\substack{m=1\\ n\neq m}}^{\mathbb{N}} x_m V_{(m),x_m}, \tag{2.16}$$

where

$$V = \sum_{n=1}^{\mathbb{N}} V_{(n)}. \tag{2.17}$$

2.1 Initial conditions and slow roll inflation

Analogous to the scalar field [7] as well as single 3-form [21, 23] inflationary models, the so-called slow roll parameters are taken as $\epsilon \equiv -\dot{H}/H^2 = -d\ln H/dN$ and $\eta \equiv \epsilon'/\epsilon - 2\epsilon$, which, for our model, are given by[3]

$$\epsilon = \frac{3}{2}\frac{\sum_{n=1}^{\mathbb{N}} V_{n,x_n}x_n}{V}\left(1-w^2\right), \tag{2.18}$$

$$\eta = \frac{\sum_{n=1}^{\mathbb{N}} x_n'\left(V_{n,x_n} + V_{n,x_n x_n}x_n\right)}{\sum_{n=1}^{\mathbb{N}} V_{n,x_n}x_n}. \tag{2.19}$$

We can see from (2.18) and (2.19) that, for $\mathbb{N}$ 3-form fields, one manner to establish a sufficient condition for inflation (with the slow roll parameters $\epsilon \ll 1$ and $\eta \ll 1$) is by means of

$$\begin{cases} 1-\sum_{n=1}^{\mathbb{N}} w_n^2 & \approx 0, \\ x_n' & \approx 0 \end{cases} \tag{2.20}$$

It is important, however, to also consider another (albeit less obvious) possibility, which is to have instead

$$\begin{cases} 1-\sum_{n=1}^{\mathbb{N}} w_n^2 \approx 0, \\ \sum_{n=1}^{\mathbb{N}} x_n'\left(V_{n,x_n} + V_{n,x_n x_n}x_n\right) & \approx 0. \end{cases} \tag{2.21}$$

The condition expressed in (2.21) means that the inclusion of more than one 3-form field allows the emergence of an inflationary scenario without even requiring that $x_n' \approx 0$. Therefore, we can expect to have different behaviors, in contrast to the ones usually found in models with just one 3-form. The different $\mathbb{N}$ 3-form fields will evolve in an intricate correlated way in order to satisfy (2.21). This possibility will deserve a more detailed analysis in the next sections. We should note that all the derived equations in this section reduce to the single one 3-form case when $\mathbb{N} = 1$, as expected.

2.2 Inflaton mass

Returning to the condition (2.20), we have

$$\sum_{n=1}^{\mathbb{N}} x_n^2 \approx \frac{2}{3\mathbb{N}}.$$

Note that the Friedman constraint (2.14) does not hold precisely at $\sum_{n=1}^{\mathbb{N}} x_n^2 = 2/3\mathbb{N}$, and $x_n' = 0$. If we assume a symmetric situation, where all w_n are equal during inflation, i.e, if all fields come to the same value during inflation, then $x_n(N)$ will take a constant value

$$x_p = \sqrt{\frac{2}{3\mathbb{N}}}. \tag{2.22}$$

In this symmetric situation, all the 3-form fields will behave identically during inflation. If $\mathbb{N}$ is very large, the plateau in x_n (N) converges towards zero ($x_p = \sqrt{\frac{2}{3\mathbb{N}}} \to 0$ as $\mathbb{N} \to \infty$, for the symmetric case where all w_n are equal). The initial conditions for the one single 3-form inflation case were discussed in [23]. The reduction of the plateau energy scale for $\mathbb{N}$ 3-forms can have a nontrivial consequence, which is to

[3] Equivalently solely in terms of $x_n$and w_n,$\eta = \frac{\sum_{n=1}^{\mathbb{N}} 3\left(\sqrt{\frac{2}{3}}w_n - x_n\right)\left(V_{n,x_n} + V_{n,x_n x_n}x_n\right)}{\sum_{n=1}^{\mathbb{N}} V_{n,x_n}x_n}$

bring the inflaton mass well below Planck mass. This is illustrated by the following analysis. Expressing the scale of the $\mathbb{N}$ 3-forms plateau (2.22) in terms[4] of the reduced Planck mass $\left(M_{\rm Pl}=1/\sqrt{8\pi G}\right)$,

$$\chi_p \approx \sqrt{\frac{2}{3\mathbb{N}}} M_{\rm Pl}, \tag{2.23}$$

let us assume that all the 3-form fields behave in the same way, reaching a constant value x_p during inflation and starting to oscillate by the end of inflation. Subsequently, we rewrite the Friedmann constraint (2.14) for this case as,

$$H^2 = \frac{1}{3}\frac{\widetilde{V}}{(1-w^2)}, \tag{2.24}$$

with $\widetilde{V}=\sum_n V_{(n)}$, $V_{(n)}=V_{0n}\, f_n\left(x_n\right)$, and where $f_n\left(x_n\right)$ are dimensionless functions. Comparing the above Eq. (2.24) with the Friedmann constraint of a single 3-form field case, we get

$$\widetilde{V} = V_1, \tag{2.25}$$

where $V_1 = V_0\, f_1(x_1)$ is the potential for the single 3-form field case. If we choose $V_{01}=V_{02}=\cdots=V_{0n}=V_{0\mathbb{N}}$, which means that the energy scales of the potentials are the same, and also assume that $x_n = x_p$ for all n in Eq. (2.25), we get

$$\frac{V_{0\mathbb{N}}}{V_0} = \frac{f_1\left(x_1\right)}{f_n\left(x_n\right)} \tag{2.26}$$

Let us consider the power law potential $f=x^l$, for a 3-form. If we substitute the corresponding value of the plateau for $\mathbb{N}$ 3-form $\left(x_p=\sqrt{\frac{2}{3\mathbb{N}}}\right)$ and of the single 3-form case $\left(x_{1p}=\sqrt{\frac{2}{3}}\right)$ in Eq. (2.26), then we can have the following ratio of energy scales for the potentials, of $\mathbb{N}$ 3-forms and single 3-form

$$\frac{V_{0\mathbb{N}}}{V_0} = \mathbb{N}^{1-\frac{l}{2}}. \tag{2.27}$$

We can translate this argument in terms of the inflaton mass, which is defined to be the square root of the second derivative of the potential. Therefore, the ratio between the inflaton masses corresponding to the $\mathbb{N}$ 3-forms potential $(m_{\mathbb{N}})$, and the single 3-form (m_1), for a power law potential $\left(x^l\right)$, is given by

$$\frac{m_{\mathbb{N}}}{m_1} \equiv \sqrt{\frac{V_{0\mathbb{N}}\, x_p^{l-2}}{V_0\, x_{1p}^{l-2}}} = \frac{1}{\mathbb{N}^{\frac{l}{2}-1}} \tag{2.28}$$

In the case of quadratic potentials ($l=2$), there is no reduction in the inflaton mass, similar to the single field case. This fact was expected since the 3-form dual action [25], when a quadratic potential is included, can be shown to be equivalent to a canonical scalar field inflation. This dual action picture enhance the fact that the 3-form inflation can encompass both features of canonical and non canonical models. In the case where $l>2$ in (2.28), it is possible to bring down the mass of the inflaton to lower energy scales by increasing the number of 3-form fields. This property opens the possibility to make a connection with particle physics since the Higgs mass was already referenced at a 125 GeV scale.

3 Two 3-form fields model

In the present section, we would like to concentrate on the case where only two 3-form fields are present [5]. Accordingly, we will rewrite some of the equations as follows. Thus, the nonzero components of Eq. (2.4) are

$$\begin{aligned} A^{(1)}_{ijk} = a^3(t)\epsilon_{ijk}X_1(t), \qquad & A^{(2)}_{ijk} = a^3(t)\epsilon_{ijk}X_2(t), \\ \Rightarrow A^2_{(1)} = 6X^2_{(1)}, \qquad & A^2_{(2)} = 6X^2_{(2)}. \end{aligned} \tag{3.1}$$

Also, we rewrite equations of motion (2.13) in terms of our dimensionless variables as

$$H^2 x_1'' + \left(3H^2+\dot{H}\right)x_1' + V^{\rm eff}_{1,x_1} = 0, \tag{3.2}$$

$$H^2 x_2'' + \left(3H^2+\dot{H}\right)x_2' + V^{\rm eff}_{2,x_2} = 0, \tag{3.3}$$

[4] An equation similar to (2.23) was also proposed to study the case of $\mathbb{N}$-flation (multiple axion inflation) model in [11]. Whereas in M-flation (Matrix inflation) there will be additional corrections, depending on $\mathbb{N}$, involved in Planck mass and arising from standard loop effects [29, 30].

[5] A generalization from two to $\mathbb{N}$ 3-form fields is left for a future work, although, whenever possible, we will point out the main aspects that can straightforwardly be generalized.

where the Friedmann and acceleration equations are given by

$$H^2 = \frac{1}{3}\frac{V_1(x_1)+V_2(x_2)}{(1-w_1^2-w_2^2)}, \tag{3.4}$$

$$\dot{H} = -\frac{1}{2}\left(V_{1,x_1}x_1 + V_{2,x_2}x_2\right). \tag{3.5}$$

In order to further discuss suitable initial conditions, the slow roll conditions $\epsilon, |\eta| \ll 1$ suggests the equation of a circle (of unit radius), as

$$w_1^2 + w_2^2 \approx 1, \tag{3.6}$$

which we rewrite in terms of trivial parametric relations as

$$\begin{aligned} w_1 &\approx \cos\theta\,, \\ w_2 &\approx \sin\theta\,. \end{aligned} \tag{3.7}$$

Subsequently, from (2.15), we can establish the initial conditions for the field derivatives

$$\begin{cases} x_1' \approx 3\left(\sqrt{\frac{2}{3}}\,\cos\theta - x_1\right), \\ x_2' \approx 3\left(\sqrt{\frac{2}{3}}\,\sin\theta - x_2\right). \end{cases} \tag{3.8}$$

Since Eq. (3.7) can be satisfied by assigning many different continuous values of the new parameter θ, we, therefore, anticipate to investigate diverse solutions. More precisely, a particular choice of this parameter will affect the way (2.19), (i.e, the value of η) will depend on the two 3-form fields. Before proceeding, let us mention that for two 3-forms inflation, we choose herein initial conditions for the fields above or below the value given by (2.22), which are expected to influence the number of e-foldings. In particular, we will investigate the asymmetric situation, when each w_n is different[6], which will provide a new behavior with respect to inflation.

3.1 Type I inflation ($x_n' \approx 0$)

As we have established in section 2.1, the slow roll conditions enable us to find two types of inflationary solutions, according to relation (2.20)-(2.21). In this subsection and the following, we investigate them in more detail. In type I solution, presented in this subsection, the 3-form fields which are responsible for driving the inflationary period, will be displaying $x_n' \approx 0$. The following is a stability analysis for this type, presented in a dynamical system context. Whenever necessary, we will complement this study by a numerical discussion.

Let us remind the autonomous system of equations for the field x_1,

$$x_1' = 3\left(\sqrt{\frac{2}{3}}w_1 - x_1\right), \tag{3.9}$$

$$w_1' = \frac{3}{2}\left(1-\left(w_1^2+w_2^2\right)\right)\left(\lambda_1\left(x_1w_1 - \sqrt{\frac{2}{3}}\right) + \lambda_2 x_2 w_1\right), \tag{3.10}$$

and also for x_2,

$$x_2' = 3\left(\sqrt{\frac{2}{3}}w_2 - x_2\right), \tag{3.11}$$

$$w_2' = \frac{3}{2}\left(1-\left(w_1^2+w_2^2\right)\right)\left(\lambda_2\left(x_2w_2 - \sqrt{\frac{2}{3}}\right) + \lambda_1 x_1 w_2\right), \tag{3.12}$$

where $\lambda_n = V_{(n),x_n}/V$. Notice that, Eqs. (3.9)-(3.10) are coupled with Eqs. (3.11)-(3.12). With the variables (x_n, w_n), let $f_1 := dx_1/dN$, $f_2 := dw_1/dN$, $f_3 := dx_2/dN$ and $f_4 := dw_2/dN$. The critical points are located at the field space coordinates (x_c) and are obtained by setting the condition $(f_1,\, f_2,\, f_3,\, f_4)|_{x_c} = 0$.

To determine the stability of the critical points, we need to perform linear perturbations around each of them by using $x(t) = x_c + \delta x(t)$; this results in the equations of motion $\delta x' = \mathcal{M}\delta x$, where $\mathcal{M}$ is

[6]For example, if we take $w_1 = 1$ and $w_{n>1} = 0$, we then find a scenario similar to one single 3-form field driving the inflation and where all the other fields approach zero.

the Jacobi matrix of each critical point whose components are $\mathcal{M}_{ij} = (\partial f_i/\partial x_j)|_{x_c}$. A critical point is called stable (unstable) whenever the eigenvalues ζ_i of $\mathcal{M}$ are such that $\mathsf{Re}(\zeta_i) < 0$ ($\mathsf{Re}(\zeta_i) > 0$) [31]. If $\mathsf{Re}(\zeta_i) = 0$, then other methods should be employed to further assess the stability of the critical point. Among different approaches, we have the center manifold theorem [32, 33, 31, 34] or, alternatively, we can consider a perturbative expansion to nonlinear order as in Refs. [35, 22]. In this work we will follow the last mentioned method, whenever necessary.

The autonomous dynamical Eqs. (3.9)-(3.12) fixed points are given by

$$\begin{aligned} x_{1c} =& \sqrt{\frac{2}{3}} w_1, \qquad & w_{1c} =& \sqrt{\frac{2}{3}} \frac{\lambda_1}{\lambda_1 x_1 + \lambda_2 x_2}, \\ x_{2c} =& \sqrt{\frac{2}{3}} w_2, \qquad & w_{2c} =& \sqrt{\frac{2}{3}} \frac{\lambda_2}{\lambda_1 x_1 + \lambda_2 x_2}. \end{aligned} \tag{3.13}$$

If $\lambda_1 \neq 0$ and $\lambda_2 \neq 0$ (otherwise, $V_{1,x_1} = 0$ and $V_{2,x_2} = 0$), Eqs. (3.13) can be rewritten as

$$\begin{aligned} x_{1c} =& \sqrt{\frac{2}{3}} w_1, \qquad & w_{1c} =& \frac{\lambda_1}{\sqrt{\lambda_1^2 + \lambda_2^2}}, \\ x_{2c} =& \sqrt{\frac{2}{3}} w_2, \qquad & w_{2c} =& \frac{\lambda_2}{\sqrt{\lambda_1^2 + \lambda_2^2}}. \end{aligned} \tag{3.14}$$

Generically, with a inflationary stage as a target, the fixed points coordinates must satisfy $w_{1c}^2 + w_{2c}^2 \simeq 1$. This last condition is required to satisfy the slow roll condition (2.20). Therefore, we can define as well

$$\begin{aligned} w_{1c} =& \cos\theta\,, \\ w_{2c} =& \sin\theta\,. \end{aligned} \tag{3.15}$$

Note that, when we consider the field coordinates in (3.13), also x_{1c} and x_{2c} are constrained by $x_{1c}^2 + x_{2c}^2 = 2/3$. Consequently, the dynamical system (3.9)-(3.12) has fixed points with only two independent degrees of freedom, which can be chosen to be the pair (x_{1c}, w_{1c}). Therefore, the critical points or inflationary attractors are found by solving the following expression $w_{1c}^2 + w_{2c}^2 = 1$, which upon substitution gives,

$$\left(\sqrt{\frac{2}{3}} \frac{\lambda_1}{\lambda_1 x_{1c} + \lambda_2 x_{2c}}\right)^2 + \left(\sqrt{\frac{2}{3}} \frac{\lambda_2}{\lambda_1 x_{1c} + \lambda_2 x_{2c}}\right)^2 = 1. \tag{3.16}$$

It is clear from the Eq. (3.16) that the location of critical points depends on the choice of 3-form potentials. For example let us take $V_1 = x_1^n$ and $V_2 = x_2^m$. It follows that

$$\left(\frac{n\left(\sqrt{\frac{2}{3}}\right)^n (\cos\theta)^{n-1}}{n\left(\sqrt{\frac{2}{3}}\cos\theta\right)^n + m\left(\sqrt{\frac{2}{3}}\sin\theta\right)^m}\right)^2 + \left(\frac{m\left(\sqrt{\frac{2}{3}}\right)^m (\sin\theta)^{m-1}}{n\left(\sqrt{\frac{2}{3}}\cos\theta\right)^n + m\left(\sqrt{\frac{2}{3}}\sin\theta\right)^m}\right)^2 = 1. \tag{3.17}$$

From Eq. (3.17), $\theta = 0$ and $\theta = \pi/2$ can be called as trivial fixed points independent of the choice of n, m. Satisfying the condition (3.17), for our particular choice of potentials, allows us to also identify non trivial fixed points in the range $0 < \theta < \pi/2$. To easily identify these, we can extract a simple constraint from Eq. (3.14), given by

$$x_{1c}/x_{2c} = \lambda_1/\lambda_2 \tag{3.18}$$

Condition (3.18) is fully consistent with Eq.(3.17), except for the trivial fixed points $\theta = 0$ and $\theta = \pi/2$. Let us apply the example where $V_1 = x_1^n$ and $V_2 = x_2^m$, and substituting in the Eq. (3.18), We have

$$\frac{n\left(\sqrt{\frac{2}{3}}\cos\theta\right)^{n-2}}{m\left(\sqrt{\frac{2}{3}}\sin\theta\right)^{m-2}} = 1\,. \tag{3.19}$$

We can read from Eq. (3.19) that for identical quadratic potentials, i.e., for $n = m = 2$, Eq. 3.18 is satisfied for all values of $0 < \theta < \pi/2$. Identical quadratic potentials is the only case where we can have an infinite number of non trivial fixed points. For any other choice of potentials , i.e., for $n \neq m$, there will only be a finite number of non trivial fixed points.

In Fig. 3.1 we illustrate the evolution of the fields x_1 and x_2 for quadratic potentials with $\theta = \pi/2$ and $\theta = \pi/4$. The asymmetry in choosing $\theta \neq \pi/4$ manifests through one of the 3-form fields having a plateau slightly higher than the other.

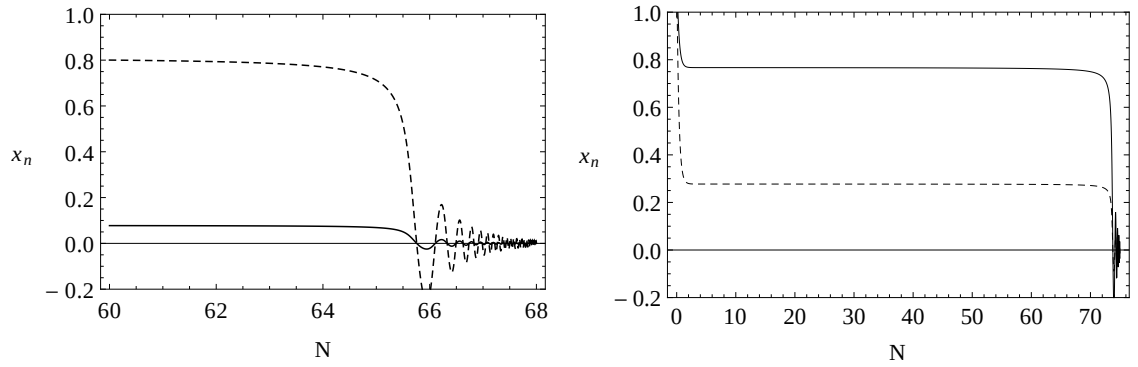


Figure 3.1: Left panel is the graphical representation of the numerical solutions of (3.2) and (3.3) for $x_1(N)$ (full line) and $x_2(N)$ (dashed line) with $\theta \approx \frac{\pi}{2}$ for the potentials $V_1 = x_1^2$ and $V_2 = x_2^2$**.** In the right panel, we depict the graphical representation of the numerical solutions of (3.2) and (3.3) for $x_1(N)$ (full line) and $x_2(N)$ (dashed line) with $\theta = \frac{\pi}{9}$. We have taken the initial conditions as $x_1(0) = 2.1 \times \sqrt{\frac{1}{3}}$ and $x_2(0) = 2.1 \times \sqrt{\frac{1}{3}}$.

Type I solutions, as far as the stability analysis, are very similar to the scenario where just one single 3-form field is present. The novelty here is that we can have solutions as shown in Fig. 3.1. Therein, we have a case where we consider that the 3-form fields x_1 and x_2 are under the influence of the same kind of quadratic potential, i.e, $V_n = x_n^2$.

We discuss the stability of these fixed points and their stability in the Appendix for simple potentials. Other combinations of potentials can be tested for stability along the same lines presented there. We summarize the results in Table 1.

$V(x_1)$	$V(x_2)$	existence	stability	Oscillatory regime
x_1^2	x_2^2	$0 < \theta < \pi/2$	unstable saddle	yes
$x_1^4 + x_1^2$	$x_2^4 + x_2^2$	$\theta = \{0, \pi/4, \pi/2\}$	unstable	yes
$x_1^3 + x_1^2$	$x_2^3 + x_2^2$	$\theta = \{0, \pi/4, \pi/2\}$	unstable	yes
$\exp\left(x_1^2\right) - 1$	$\exp\left(x_2^2\right) - 1$	$\theta = \{0, \pi/4, \pi/2\}$	unstable	yes
x_1^2	$x_2^4 + x_2^2$	$\theta = \{0, \pi/2\}$	unstable	yes
$\exp\left(-x_1^2\right)$	$\exp\left(-x_2^2\right)$	$\theta = \{0, \pi/4, \pi/2\}$	unstable	no
x_1^2	x_2^4	$\theta = \{0, \pi/3, \pi/2\}$	unstable	yes
$x_1^n \quad (n > 2)$	$x_2^n \quad (n > 2)$	$\theta = \{0, \pi/4, \pi/2\}$	unstable	no

Table 1: Summary of some type I solutions critical points and their properties.

3.2 Type II inflation ($x_n' \not\approx 0$)

Let us now present the other class of inflationary solution, which was mentioned in the Introduction. This type is associated to the manner asymmetry is present. Let us be more specific. One way to attain this solution consists of choosing an initial value of θ away from the fixed points previously discussed. This corresponds to the curved trajectories in the right panel of Fig.3.3. Another is by choosing different sclales of the potentials. In any case, the inflationary behavior (type II) is similarly affected concerning either way of introducing asymmetry. We should note here that there is no analog for a type II solution within single 3-form driven inflation. To understand this new type of inflationary scenario, let us take $V_1 = x_1^2$ and $V_2 = 2x_2^2$ (just different slopes), whose numerical solutions are plotted in Fig. 3.2.

In Fig. 3.2, the two fields continuously evolve, and at the same time assist each other in order to sustain a slow roll regime. As we can see from the left panel of Fig. 3.2, one field continues to slowly decrease (dashed line) and the other (full line) starts to increase until it enters in an oscillatory regime. However, in the right panel of Fig. 3.2, we see that the slow roll parameters evolve (before oscillating) near to zero during the period of inflation. Moreover, from Eq. (2.19), the behavior of the two fields are such that even with $x_n' \not\approx 0$, the slow roll conditions are consistent with inflation. The fact is that the

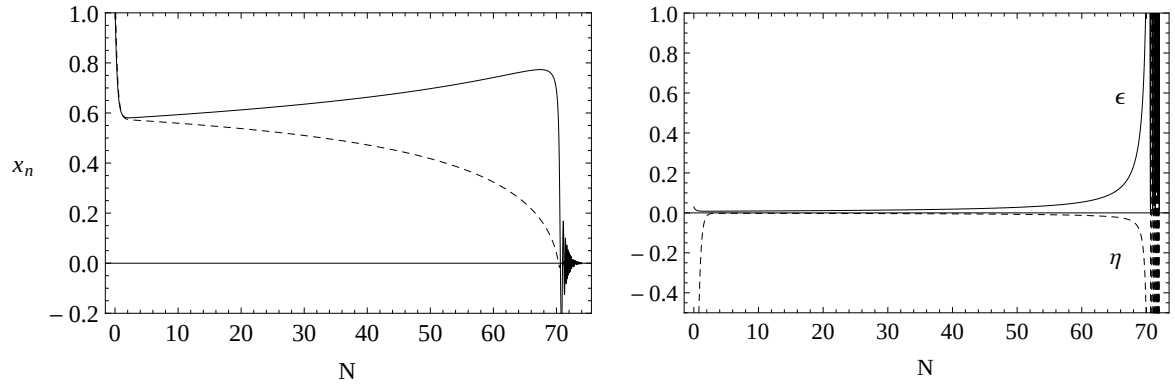


Figure 3.2: In the left panel we have the graphical representation of the numerical solutions of (3.2) and (3.3) for $x_1(N)$ (full line) and $x_2(N)$ (dashed line) with $\theta = \frac{\pi}{4}$ for the potentials $V_1 = x_1^2$ and $V_2 = 2x_2^2$. We have taken the initial conditions as $x_1(0) = 1.8 \times \sqrt{\frac{1}{3}}$ and $x_2(0) = 2.0 \times \sqrt{\frac{1}{3}}$. In the right panel, and for the same initial conditions, we have the graphical representation of the numerical solutions for $\epsilon(N)$ (full line) and $\eta(N)$ (dashed line).

slow roll parameter $\eta \to 0$ is now due to the constraint (2.21). As previously mentioned, a rather unusual cooperation between the two 3-form fields, emphasized by the mentioned coupling (gravity mediated, through $\dot{H}$) provides a different inflationary dynamics.

This new type of solution presents a period of inflation with an interesting new feature. More precisely, when one 3-form field decreases, say x_1, then the other field, x_2, is constrained to increase. However, the increase of the second 3-form field is limited by the fact that, as the first one inevitably approaches zero, then Eq. (3.12) becomes

$$w_2' \sim \frac{3}{2}\left(1 - w_2^2\right)\lambda_2\left(x_2 w_2 - \sqrt{\frac{2}{3}}\right), \tag{3.20}$$

with the coupling term $\lambda_1 x_1 w_2$ being negligibly small. We see that Eq. (3.20) will become zero when w_2 (which is increasing, as is x_2) will approach 1. At this stage, and inspecting Eq. (3.11), it is clear that x_2 will stop increasing and start to decrease, making $x_2' < 0$. This situation is depicted in the left panel Fig. 3.2, where the decreasing field is reaching zero at the same period where the other stops to increase and also converges to zero. The two 3-form fields behave strongly correlated and assisting each other through the inflationary period. Therefore, this more complex and correlated evolution of the fields can provide a different observational signature when compared to other multifield inflationary models.

The different nature of type I and type II solutions is be represented in Fig. 3.3. Therein, we have a parametric plot[7] of $x_1(N)$ and $x_2(N)$ in the field space, where the fixed points (cf. in particular the analysis in A.1 and A.2) are located at a pair of coordinates (x_{1c}, x_{2c}), of course associated to a situation where $(x_1', x_2') = 0$.

The two fields rapidly evolve towards this pair of coordinates, (cf. the behavior illustrated in Figs. 3.1 and 3.2) settling there for the inflationary period. Afterwards, and because these fixed points are not stable, the two fields will eventually diverge from it. More precisely, in the left panel of Fig. 3.3 we have the particular case where the two 3-form fields are under the influence of identical quadratic potentials. In this case, only type I solutions are present and the inflationary epochs, occur near the depicted circle. Those fixed points in this figure are all located in the arc of radius $\sqrt{2/3}$ in the (x_1, x_2) plane. The right panel, of the same figure, constitutes an example where only one fixed point is present (using Eq. (3.17)) between $\theta = 0$ and $\theta = \pi/2$. This fixed point, located at (C) in the right panel, corresponds to a type I solution when $\theta = \pi/3$, for a case where the potentials are $V(x_1) = x_1^2$ and $V(x_2) = x_2^4$. All the other depicted trajectories are type II solutions, where the $\dot{H}$-term coupling mediation plays a crucial role(cf. Fig 3.2). The peculiar oscillatory regime, present the right panel of 3.3, is also characteristic of the coupling term in the effective potential (2.11). We shall discuss the oscillatory behavior in the following subsection.

3.2.1 Oscillatory regime after inflation

The main purpose of this section is to present an analytical description of the oscillatory behavior, emerging by the end of inflation for the choice of potentials presented in Table 1. This analysis can also

[7]Please note that Fig. 3.3 is *not* a phase space representation.

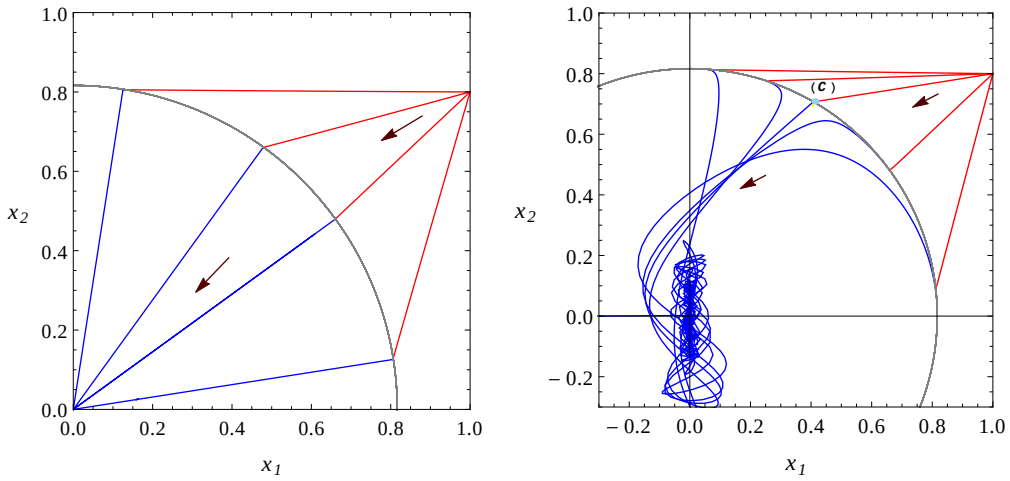


Figure 3.3: This figure represents a set of trajectories evolving in the (x_1, x_2) space. These trajectories are numerical solutions of (3.2) and (3.3) and correspond to a situation where we choose $V_1 = x_1^2$ and $V_2 = x_2^2$ (left panel), as an illustrative example only showing type I solution. All the fixed points are part of the arc of radius $\sqrt{2/3}$ in the (x_1, x_2) plane. In the right panel, we have an example, where we have taken $V_1 = x_1^2$ and $V_2 = x_2^4$, showing type II solutions, except for the trajectory going close to a fixed point with $\theta = \pi/3$ (point C). In addition, in the right panel, we have an illustration of two 3-form fields damped oscillations by the end of inflation. The arrows, in the plots, indicate the direction of time in the trajectories.

be useful for subsequent studies on reheating and particle production, as modeled by the two 3-forms scenario which we postpone for a future work. The interesting aspect that happens with two 3-forms is due to the presence of the $\dot{H}$ coupling term in the effective potential (2.10), which becomes particularly dominant and produces a nontrivial interaction between the 3-form fields in the type II case. At this point, we must note that this property is more general, in the sense that the conclusion drawn for two fields can be easily extended when more 3-form fields are included. The choice of potential plays an important role regarding the presence of a consistent oscillatory behavior, which successfully avoid ghost instabilities by the end of inflation. This is illustrated for single 3-form inflation in the Ref. [23, 24]. Based on the studies of single 3-form inflation, we chose potentials containing quadratic behavior. Moreover, we must emphasize that the oscillatory regime for two 3-forms case is different from single 3-form inflation, due to the presence of the coupling term in the equations of motion. An exception is the case of identical quadratic potentials, i.e., taking $V_{(n)} = x_n^2$, where we can reasonably ignore the effect of coupling. This is the special case where two 3-form fields oscillate almost independently.

To illustrate this, let us first consider that the two fields are subjected to quadratic potentials $V_{(n)} = \frac{1}{2}m_n^2\chi_n^2$. For simplicity we work with the equations of motion in t time (2.5). The equation of motion (2.5) for the 3-form field χ_n can be approximated in the small field limit ($\chi_n \to 0$) by neglecting the effect of coupling term in the effective potential (2.11) as,

$$\ddot{\chi}_n + 3H\dot{\chi}_n + m_n^2\chi_n \approx 0. \tag{3.21}$$

From the Friedmann constraint (2.6) we have that during inflation H slowly decreases, since $\dot{H} < 0$. When inflation ends, $m_n^2 \sim H^2$, and subsequently the 3-form fields begin to coherently oscillate at scales $m_n^2 \gg H^2$. The evolution of χ_n at the oscillatory phase can be studied by changing the variable $\chi_n = a^{-3/2}\bar{\chi}_n$, so that Eq. (3.21) becomes

$$\ddot{\bar{\chi}}_n + \left(m_n^2 - \frac{9}{4}H^2 - \frac{3}{2}\dot{H}\right)\bar{\chi}_n \approx 0 \tag{3.22}$$

Using the approximations $m_n^2 \gg H^2$ and $m_n^2 \gg \dot{H}$, the solution to the Eq. (3.22) can be written as

$$\bar{\chi}_n = C\sin(m_n t) \tag{3.23}$$

where C is a the maximum amplitude of the oscillations. Thus the solution for χ_n can be written as

$$\chi_n = Ca^{-3/2}\sin(m_n t)\,. \tag{3.24}$$

An interesting aspect arises in the small field limit when one of the two 3-form fields potentials is not quadratic. Let us suppose the situation described in A.2, with one field subjected to a quartic potential,

$V_2 = \lambda\chi_2^4$. This discussion is related to the oscillatory phase we see in the right panel of Fig. 3.3, regarding the type II case. This combination of potentials has the peculiar feature to induce an oscillatory regime, more precisely, that for a single 3-form field it would be absent under the quartic potential due to the presence of a ghost term [23]. In the limit $\chi_1,\, \chi_2 \to 0$, towards the oscillatory phase, the field χ_1 will be approximately described by Eq. (3.24). Therefore the 3-form field χ_1 undergoes a damped oscillatory regime due to the dominance of quadratic behavior. However, the second field χ_2, also undergoes an oscillatory regime, not caused by the quartic potential but due to the coupling term, $V^{\rm eff}_{2,x_2}$, dominance in Eq. (3.3). The equation of motion (3.2) for the 3-form field becomes (in the small field limit, $\chi_1,\, \chi_2 \to 0$, near the oscillatory phase),

$$\ddot{\chi}_2 + 3H\dot{\chi}_2 + \left(4\lambda\chi_2^3 - \frac{3}{2}m_1^2\chi_1^2\chi_2\right) \approx 0. \tag{3.25}$$

The nonlinear differential equation (3.25) is explicitly affected by the oscillatory behavior of χ_1, which could cause something similar to a parametric resonance effect in particle production [24]. The effective potential also carries a cubic term, which turns the equation difficult to solve. However, we can conjecture that for two 3-forms inflation, at least one of the potentials must contain a quadratic behavior, which forces all the other fields to undergo a consistent oscillatory phase due to the influence of the coupling term. In the case of the single 3-form inflation, there is no oscillatory behavior for quartic potential, a fact that the authors in [23] explain by means of ghost instabilities. Therefore, to conclude this section we present a new choice of potential i.e., $V_1 = x_1^2$ and $V_2 = x_2^4$, which can avoid ghost instabilities due to the presence of consistent oscillatory phase. A similar oscillatory regime is present when assisted inflation with two scalar fields is studied by means of an explicit quartic coupling in the action [36].

3.2.2 Varying speed of sound for two 3-form fields

In the following we examine how the type II solutions establish pressure perturbations with varying speed of sound.

Adiabatic perturbations are defined by

$$\frac{\delta p}{\dot{p}} = \frac{\delta\rho}{\dot{\rho}}$$

where p and ρ are the pressure and energy density of the system. Pressure perturbations can in general be expanded as a sum of an adiabatic and a non adiabatic perturbations (δp_{nad}), which is given by [37]

$$\delta p = \delta p_{\rm nad} + c_s^2\delta\rho$$

where $c_s^2 = \dot{p}/\dot{\rho}$ is the adiabatic sound speed for scalar perturbations in a thermodynamic system. The distinction between adiabatic sound speed and phase sound is given for scalar field models in Ref. [38]. When an adiabatic system is composed with multiple scalar fields ϕ_n, we have that

$$\frac{\delta\phi_i}{\dot{\phi}_i} = \frac{\delta\phi_j}{\dot{\phi}_j}. \tag{3.26}$$

The condition (3.26) is consequently valid for any two scalar field systems. The above condition can also be applicable for a system of $\mathbb{N}$ 3-forms because its action can (at least formally) always be dualized and reduced to an action with $\mathbb{N}$ non canonical scalar fields [25].

The general expression for the adiabatic sound speed for $\mathbb{N}$ 3-form fields is defined as

$$c_s^2 = \frac{\dot{p}_{\mathbb{N}}}{\dot{\rho}_{\mathbb{N}}}. \tag{3.27}$$

If we take (2.8) and (2.9) within the slow roll approximation $\chi_n'' \ll V_n(\chi_n)$, we get, generally

$$c_s^2 = \frac{\sum_{n=1}^{\mathbb{N}} \chi_n'\, \chi_n\, V_{,\chi_n\chi_n}}{\sum_{n=1}^{\mathbb{N}} \chi_n'\, V_{,\chi_n}} \tag{3.28}$$

Which, in the two 3-forms case, allows the speed of sound to be explicitly written as

$$c_s^2 = \frac{\chi_1'\,\chi_1\,V_{,\chi_1\chi_1} + \chi_2'\,\chi_2\,V_{,\chi_2\chi_2}}{\chi_1'\,V_{,\chi_1} + \chi_2'\,V_{,\chi_2}}$$

Unlike the one 3-form sound speed, in a two 3-forms setting the sound speed will depend on χ_n'. For type I inflation, for which we have ($\chi_n' \approx 0$), the speed of sound (3.28) becomes constant during inflation. For the type II solution, where we have $\chi_n' \not\approx 0$, the speed of sound, c_s^2, can vary during the inflationary period. This varying speed can subsequently exhibit a peculiar imprint in the primordial power spectrum,

scale invariance and bi-spectrum extracted from the CMB data. We are going to explore, in the next two sections, observational consequences, due to a varying speed of sound, upon important quantities like the tensor-scalar ratio, spectral index and running spectral index, by examining particular type II solutions for suitable choice of potentials.

4 Isocurvature perturbations and primordial spectra

One important feature of multiple field models is the generation of isocurvature perturbations. In this section we examine the effect of these perturbations in the context of two 3-form fields scenario. More concretely, we will distinguish, type I and type II solutions, with respect to the evolution of isocurvature perturbations.

As depicted, in the right panel of Fig. 3.3 type I solutions are characterized by a straight line, whereas type II solutions follow a curved trajectory in field space. In scalar multifield models, a local rotation in the field space is carried to define the adiabatic and entropy modes (or fields [39]). In order to express these adiabatic and entropy fields from two 3-form fields, the first step consists in defining a dual scalar field Lagrangian for the two 3-forms (see Ref. [25]). The second step consists in applying the general framework of adiabatic and entropy perturbations to our model. We start by presenting the $\mathbb{N}$ 3-forms Lagrangian in terms of a non canonical Lagrangian $P(X,\phi_n)$, where[8] $X=-\frac{1}{2}\partial^\mu\phi_n\partial_\mu\phi_n$[9], and ϕ_n is the dual scalar field corresponding to the 3-form field tensor $F_{\alpha\beta\gamma\delta}$. The motivation to work with the dual action is related to the fact that the general framework of adiabatic and entropy perturbations for the non canonical multifield model has already been consistently established. In the following we will briefly review and adopt to our case the results described previously in [26, 10, 25, 40, 41].

The action for the dual scalar fields representation of the $\mathbb{N}$ 3-forms can be written as [25],

$$P(X,\phi_n)=\sum_{n=1}^{\mathbb{N}}\left(\chi_n V_{n,\chi_n}-V(\chi_n)-\frac{\phi_n^2}{2}\right), \tag{4.1}$$

with

$$X=\sum_n X_n, \qquad \text{and} \qquad X_n=\frac{1}{2}V_{n,\chi_n}^2. \tag{4.2}$$

In the above equations, χ_n represent one element of the $\mathbb{N}$ 3-form fields (cf. eqs. (2.3)-(2.5)). In the Lagrangian (4.1) we can identify the kinetic term to be

$$K_n(X_n)=\sum_{n=1}^{\mathbb{N}}\left(\chi_n V_{n,\chi_n}-V(\chi_n)\right). \tag{4.3}$$

Since this kinetic term is only a function of X_n and not of ϕ_n, this means that the field metric is $G_{nm}(\phi)=\delta_{nm}$. Restricting ourselves now to a two 3-form scenario, and according to [39], we can define the adiabatic and entropy fields through a rotation in the two 3-form dual field space,

$$\dot\sigma=\sqrt{2X_1}\cos\Theta+\sqrt{2X_2}\sin\Theta \tag{4.4}$$

$$\dot s=-\sqrt{2X_1}\sin\Theta+\sqrt{2X_2}\cos\Theta \tag{4.5}$$

where $\tan\Theta=\sqrt{X_2}/\sqrt{X_1}$, $X_1=\frac{1}{2}V_{1,\chi_1}^2$ and $X_2=\frac{1}{2}V_{2,\chi_2}^2$. Subsequently, the adiabatic and entropy perturbations are

$$Q_\sigma=\delta\phi_1\cos\Theta+\delta\phi_2\sin\Theta \tag{4.6}$$

$$Q_s=-\delta\phi_1\sin\Theta+\delta\phi_2\cos\Theta, \tag{4.7}$$

respectively, along and orthogonal to the background classical trajectory in dual field space.

Let us assume that the linearly perturbed metric is given by

$$ds^2=-(1+2\varphi)dt^2+2\partial_i\beta dx^i dt+a^2(t)\left(1-2\psi\right)dx^2$$

We have chosen a flat gauge, where the dynamics of linear perturbations are completely expressed in terms of the scalar field perturbations ($\phi^n\to\phi_0^n+Q^n$). Moreover, these are defined as gauge invariant combinations given by $Q^n=\delta\phi^n+(\phi^n/H)\,\psi$. The comoving curvature perturbation is given by

$$\mathcal{R}\equiv\psi-\frac{H}{p+\rho}\delta q\,, \tag{4.8}$$

[8]The notation "n" indicating n^{th}field here corresponds to "I" in Ref.[26]

[9]Note that in the Ref.[25] the definition $X=-\partial^\mu\phi_n\partial_\mu\phi_n$ differs by a 2 factor from our notation. Accordingly, we have considered this difference throughout this section.

where $\partial_i \delta q_i = \delta T_i^0$ and $\mathcal{R}$ purely characterizes the adiabatic part of the perturbations. The variation of $\mathcal{R}$, in the flat gauge, is given by [26]

$$\dot{\mathcal{R}} = \frac{H}{\dot{H}} \frac{c_s^2 k^2}{a^2} \Psi + \frac{H}{\dot{\sigma}} \Xi Q_s \quad \text{with} \quad \Xi = \frac{1}{\dot{\sigma} P_{,X}} \left(\left(1 + c_s^2\right) P_{,s} - c_s^2 \dot{\sigma}^2 P_{,Xs} \right), \tag{4.9}$$

where Ψ is the Bardeen potential and

$$P_{,s} = P_{,X} \dot{\sigma} \dot{\Theta}, \qquad \begin{pmatrix} P_{,X\sigma} \\ P_{,Xs} \end{pmatrix} = \begin{pmatrix} \cos\Theta & \sin\Theta \\ -\sin\Theta & \cos\Theta \end{pmatrix} \begin{pmatrix} P_{,X_1} \\ P_{,X_2} \end{pmatrix}. \tag{4.10}$$

For a two 3-form dual Lagrangian, extracted from (4.1), we can express the above quantities as functions of the 3-form fields, i.e.,

$$P_{,X} \equiv P_{,X_1} + P_{,X_2} = \frac{\chi_1}{V_{1,\chi_1}} + \frac{\chi_2}{V_{2,\chi_2}} \tag{4.11}$$

Using Eqs. (4.11) and (4.10) we can simplify Ξ, to obtain,

$$\Xi = H \left(\left(1 + c_s^2\right) \frac{d\Theta}{dN} - c_s^2 \frac{\dot{\sigma}}{H} \frac{P_{,Xs}}{P_{,X}} \right). \tag{4.12}$$

The function Ξ is a measure of the coupling between the entropy and adiabatic modes.

4.1 Type I inflation

In type I inflationary scenarios, where $\dot{\Theta} = 0$ (as $\tan\Theta = \lambda_2/\lambda_1 = x_2/x_1 =$ constant in the fixed point, cf. Eq.(3.14) and see Fig. 3.3), the classical trajectory is a straight line. This fact makes the first term of Ξ, in Eq. (4.12), to vanish.

On the other hand, the ratio $P_{,Xs}/P_{,X}$ can be expressed as

$$\frac{P_{,Xs}}{P_{,X}} = \frac{-\chi_1 \sin\Theta + \chi_2 \cos\Theta}{\chi_1 V_{1,\chi_1} + \chi_2 V_{2,\chi_2}}. \tag{4.13}$$

Expression (4.13) vanishes for all type I solutions since $\chi_2 = \chi_1 \left(\lambda_2/\lambda_1\right) = \chi_1 \tan\Theta$. In other words, there are no entropy perturbations sourcing the curvature perturbations. We then recover the known relation for a single field inflation

$$\dot{\mathcal{R}} = \frac{H}{\dot{H}} \frac{c_s^2 k^2}{a^2} \Psi, \tag{4.14}$$

and we can state that the curvature perturbation is conserved on the large scales. We can, therefore, compute the power spectrum of curvature perturbations in terms of quantities values at horizon exit.

4.2 Type II inflation

For type II inflation, the aforementioned effects, namely of entropy perturbations, can be present due to the curved trajectory (cf. the right panel of Fig.3.3) in field space ($\dot{\Theta} \neq 0$). Due to this the curvature power spectrum could be sourced by entropy perturbations on large scales.

In order to study quantum fluctuations of the system we must consider the following canonically normalized fields defined by,

$$v_\sigma = \frac{a\sqrt{P_{,X}}}{c_s} Q_\sigma, \qquad v_s = a\sqrt{P_{,X}} Q_s \,,$$

we can express the second order action for the adiabatic and entropy modes as

$$S_{(2)} = \frac{1}{2} \int d\tau d^3k \left[v_\sigma'^2 + v_s'^2 - 2\xi v_\sigma' v_s - k^2 c_s^2 v_\sigma^2 - k^2 v_s^2 + \Omega_{\sigma\sigma} v_s^2 + \Omega_{ss} v_\sigma^2 + 2\Omega_{s\sigma} v_\sigma v_s \right] \tag{4.15}$$

with

$$\xi = \frac{a}{c_s} \Xi, \quad \Omega_{\sigma\sigma} = \frac{z''}{z} \quad \text{and} \quad \Omega_{ss} = \frac{\alpha''}{\alpha} - a^2 \mu_s^2,$$

where z and α are background dependent functions defined by

$$z = \frac{a\dot{\sigma}\sqrt{P_{,X}}}{c_s H}, \; \alpha = a\sqrt{P_{,X}} \,.$$

The equations of motion derived from the action (4.15) are given by

$$v_\sigma'' - \xi v_s' + \left(c_s^2 k^2 - \frac{z''}{z}\right) v_\sigma - \frac{(z\xi)'}{z} v_s = 0\,, \tag{4.16}$$

$$v_s'' + \xi v_\sigma' + \left(k^2 - \frac{\alpha''}{\alpha} + a^2\mu_s^2\right) v_s - \frac{z'}{z}\xi v_\sigma = 0\,, \tag{4.17}$$

where μ_s^2 is the effective mass for the entropy field given by [26]

$$\mu_s^2 = -\frac{P_{,ss}}{P_{,X}} - \frac{1}{2c_s^2\,(X_1+X_2)}\frac{P_{,s}^2}{P_{,X}^2} + 2\frac{P_{,Xs}P_{,s}}{P_{,X}^2} \tag{4.18}$$

and

$$\begin{pmatrix} P_{,\sigma\sigma} & P_{,\sigma s} \\ P_{,s\sigma} & P_{,ss} \end{pmatrix} = \begin{pmatrix} \cos\Theta & \sin\Theta \\ -\sin\Theta & \cos\Theta \end{pmatrix} \begin{pmatrix} P_{,X_1X_1} & P_{,X_1X_2} \\ P_{,X_2X_1} & P_{,X_2X_2} \end{pmatrix} \begin{pmatrix} \cos\Theta & -\sin\Theta \\ \sin\Theta & \cos\Theta \end{pmatrix} \tag{4.19}$$

The coupling between adiabatic and entropy modes is governed by the parameter ξ. In the cases where this parameter can be assumed to be small (see [26, 10]) at the typical scale of sound horizon exit [10] the adiabatic and entropy modes decouple and analytical solutions for Eqs. (4.16)-(4.17) can easily be found. In the decoupled case the adiabatic and entropy modes evolve according to the following equations,

$$v_\sigma'' - \left(c_s^2 k^2 - \frac{z''}{z}\right) v_\sigma = 0, \tag{4.20}$$

$$v_s'' + \left(k^2 - \frac{\alpha''}{\alpha} + a^2\mu_s^2\right) v_s = 0. \tag{4.21}$$

In the slow roll limit, for a speed of sound that slowly varies while the scales of interest cross out the sound horizon, we can assume $z^{''}/z^{'} = 1/\tau^2$. Using this, we get as a general approximate solutions for the adiabatic and entropy modes with Bunch-Davies vacuum initial conditions,

$$v_{\sigma k} \simeq \frac{1}{\sqrt{2kc_s}} \exp\left(-ikc_s\tau\right)\left(1 - \frac{i}{kc_s\tau}\right), \tag{4.22}$$

$$v_{sk} \simeq \frac{1}{\sqrt{2k}} \exp\left(-ik\tau\right)\left(1 - \frac{i}{k\tau}\right), \tag{4.23}$$

where we assume $\frac{\mu_s^2}{H^2} \ll 1$ is valid for our case. This means entropy modes get amplified with respect to the adiabatic modes at the sound horizon crossing

$$Q_{\sigma_*} \simeq \frac{Q_{s_*}}{c_{s_*}}. \tag{4.24}$$

The curvature and isocurvature perturbations are respectively,

$$\mathcal{R} = \frac{H}{\dot\sigma} Q_\sigma, \qquad \mathcal{S} = c_s \frac{H}{\dot\sigma} Q_s \tag{4.25}$$

The power spectrum of the curvature perturbation, evaluated at the sound horizon crossing ($c_s k = aH$), is given by

$$\mathcal{P}_{\mathcal{R}_*} = \frac{k^3}{2\pi^2}\frac{|\,v_{\sigma k}\,|^2}{z^2} \simeq \frac{H^4}{8\pi^2 X P_{,X}} = \left.\frac{H^2}{8\pi^2\epsilon c_s}\right|_*, \tag{4.26}$$

which recovers with the single field power spectrum result at horizon crossing [25]. However, in contrast to the single field inflation, the function ξ is not negligible and typically varies with time. This means that there will be a transfer between entropic and adiabatic modes on large scales but the converse is not true. From Eqs. (4.9) and (4.25), the evolution of the curvature and entropy modes in the long wavelength limit can be approximated as [40]

$$\dot{\mathcal{R}} \approx \alpha H S, \qquad \dot{\mathcal{S}} \approx \beta H S,$$

[10] In contrast to the inflationary models where a sharp turn in field space occurs during inflation [42, 43, 44].

where the coefficients α and β are taken to be,

$$\alpha = \frac{\Xi}{c_s H}, \tag{4.27}$$

$$\beta \simeq \frac{s}{2} - \frac{\eta}{2} - \frac{1}{3H^2}\left(\mu_s^2 + \frac{\Xi^2}{c_s^2}\right), \tag{4.28}$$

endowed with the definition of an additional slow roll parameter $s = \frac{\dot{c}_s}{Hc_s}$. The evolution of curvature and isocurvature perturbations after horizon crossing can be evaluated using transfer functions defined by

$$\begin{pmatrix} \mathcal{R} \\ \mathcal{S} \end{pmatrix} = \begin{pmatrix} 1 & \mathcal{T}_{\mathcal{RS}} \\ 0 & \mathcal{T}_{\mathcal{SS}} \end{pmatrix} \begin{pmatrix} \mathcal{R} \\ \mathcal{S} \end{pmatrix}_*,$$

where

$$\mathcal{T}_{\mathcal{RS}}(t_*, t) = \int_{t_*}^{t} dt' \alpha(t') H(t') T_{SS}(t_*), \tag{4.29}$$

and

$$\mathcal{T}_{\mathcal{SS}}(t_*, t) = \exp\left\{\int_{t_*}^{t} dt' \beta(t') H(t') dt'\right\}, \tag{4.30}$$

In addition, the curvature perturbation power spectrum, the entropy perturbation and the correlation between the two can be formally related as

$$\mathcal{P}_{\mathcal{R}} = \left(1 + \mathcal{T}_{\mathcal{RS}}^2\right)\mathcal{P}_*, \qquad \mathcal{P}_{\mathcal{S}} = \mathcal{T}_{\mathcal{SS}}^2 \mathcal{P}_*, \tag{4.31}$$

$$\mathcal{C}_{\mathcal{RS}} \equiv \langle \mathcal{RS} \rangle = \mathcal{T}_{\mathcal{RS}} \mathcal{T}_{\mathcal{SS}} \mathcal{P}_*. \tag{4.32}$$

In contrast to the power spectrum for the scalar perturbations, the tensor power spectrum amplitude is the same as for a single field,

$$\mathcal{P}_{\mathsf{T}} = \frac{2}{\pi^2}\frac{H^2}{M_{PI}^2}\bigg|_*.$$

The tensor scalar ratio defined in multifield inflation is given by

$$r \equiv \frac{\mathcal{P}_{\mathsf{T}}}{\mathcal{P}_{\mathcal{R}}} = 16\epsilon c_s \bigg|_* \cos^2\Delta, \tag{4.33}$$

where Δ is the transfer angle given by

$$\cos\Delta = \frac{1}{\sqrt{1 + \mathcal{T}_{\mathcal{RS}}^2}}.$$

Similarly, the spectral index also gets a correction, provided by the transfer functions,

$$n_s \equiv \frac{d \ln \mathcal{P}_{\mathcal{R}}}{d \ln k} = n_s(t_*) + \frac{1}{H_*}\left(\frac{\partial T_{RS}}{\partial t_*}\right)\sin(2\Delta), \tag{4.34}$$

where

$$n_{s_*} = 1 - 2\epsilon_* - \eta_* - s_*.$$

The spectral index and the tensor to scalar ratio are the key observables which not only depend on the slow roll at horizon crossing, but also depend on the transfer angle Δ. This enables a clear distinction between multifields and single field inflationary scenarios [11] [45]. The transfer functions defined in Eqs. (4.29) and (4.30) are allowed to evolve after the Hubble exit, even after inflation, during the reheating and radiation dominated era [45, 47]. However the evolution of isocurvature perturbations, during reheating and radiation dominated era, would depend on the particular final stage of the inflationary scenario. Consider for example, a two field scenario, if one field enters a regime of oscillations while the second field is still inflating the Universe. In such cases the curvature perturbation can be sourced by entropy modes even after inflation [46]. This kind of scenarios are known as 'curvaton' or 'spectator' field behavior [48, 49] and also found in double quadratic inflation [47]. In the case of two 3-forms inflation, we will assume that entropy perturbations do not grow further after inflation. Therefore we only evaluate transfer functions from horizon exit until the end of inflation and predict the values of n_s and r [43]. We can see from Eqs. (4.33) and (4.34) that if $\mathcal{T}_{\mathcal{RS}} = 0$ then our predictions match the single field result. From the section 4.1 and Eq. 4.27 it is evident that $\mathcal{T}_{\mathcal{RS}} = 0$ for type I inflation. Therefore to make observational contrast with single 3-form we mainly focus on testing type II inflationary scenario in the following section.

[11] However tensor scalar ratio is more constrained by consistency relations in case of inflation with more than two fields [45, 46].

5 Two 3-form fields inflation and observational data

Based on the discussion made on the curvature perturbation power spectrum in section 4, the main objective is to test our two 3-forms model and predicting values of inflationary parameters. We choose suitable potentials and initial conditions, in order to obtain a reasonable fit with present available experimental bounds [1, 28]. The majority of inflationary models with a non canonical kinetic term contain a common feature that the adiabatic fluctuations propagate with a sound speed $c_s^2 < 1$. The recent Planck data restricts this speed of sound to be in the interval $0.02 \lesssim c_s^2 < 1$. Multiple field inflation models allow the possibility of having a varying speed of sound, i.e, like for the type II solution in our model (cf. section 3.2.2). The speed of sound variation will therefore have implications on the running spectral index and the scale invariance. These peculiar effects, being a consequence of the varying speed of sound, have been studied in a DBI context and also in modified gravity models with an effective inflaton [50, 51, 52].

We have examined all the potentials in Table 1. We found that $\chi_i^2 + b_i\chi_i^4$ is consistent with observational bounds[12]. It is quite difficult to constrain the speed of sound $\left(0.02 \lesssim c_s^2 < 1\right)$ during inflation. We found that only type II solutions which are slightly deviated from type I are suitable to maintain consistent speed of sound during inflation. To predict values of inflationary parameters, first we need to compute the transfer functions defined in section 4 and evaluate their value at the end of inflation.

We can read from Eq. (4.34) that the spectral index depends on the derivative of $\mathcal{T}_{\mathcal{RS}}$ at horizon crossing. From the right panel of Fig. 5.1 it is clear that the derivative of $\mathcal{T}_{\mathcal{RS}}$, between $N = 0$ and $N = 20$, is very small and we can, therefore, neglect it. Hence, our prediction of spectral index only depends on the values of the slow roll parameters at horizon exit.

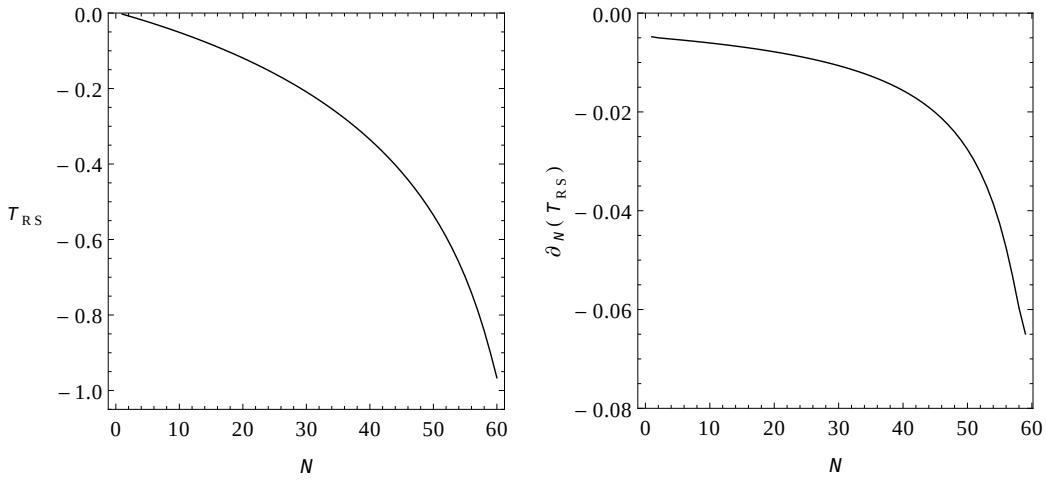


Figure 5.1: Graphical representation of $\mathcal{T}_{\mathcal{RS}}$ (left panel) and $\frac{d\mathcal{T}_{\mathcal{RS}}}{dN}$ (right panel) till the end of inflation (defined for $\epsilon = 1$). We have taken $V_1 = V_{10}(x_1^2 + bx_1^4)$ and $V_2 = V_{20}(x_2^2 + bx_2^4)$ where $V_{10} = 1$, $V_{20} = 0.93$, $b = -0.35$ and with initial conditions $\theta = \pi/4$.

The running of the spectral index to the lowest order in slow roll is now given by, regime,

$$\frac{dn_s}{d\ln k} = \quad = \left(1 + \epsilon + \frac{c_s'}{c_s}\right)\Bigg|_* \left(n_{s_*}' + \frac{\partial \mathcal{T}_{\mathcal{RS}}}{\partial N_*}\frac{\partial}{\partial N}\left(\frac{2\mathcal{T}_{\mathcal{RS}}}{1+\mathcal{T}_{\mathcal{RS}}^2}\right) + \frac{\partial^2 \mathcal{T}_{\mathcal{RS}}}{\partial N_*^2}\sin 2\Delta\right). \tag{5.1}$$

For the choice of potential in Fig. 5.1 we can neglect the transfer function corrections to the running spectral index (5.1). Therefore for this case the additional slow roll parameter $s = \frac{c_s'}{c_s}$ is of relevance, which enables us to observationally distinguish between two 3-forms and single 3-form inflation[13], with respect to the running of spectral index. Expression (5.1) is expanded up to the first order in the slow roll parameters. The second order corrections are crucial if there is an abrupt path turn in field space during horizon exit. These types of scenarios are considered in detail in studies related with hybrid inflation and double quadratic inflation [53]. We can neglect these corrections for two 3-form inflation, since the type II solutions herein considered do not exhibit abrupt turns in field space under slow roll conditions.

To predict tensor scalar ratio (4.33) for two 3-forms it is required to know the value of $\mathcal{T}_{\mathcal{RS}}$ at the end of inflation. From the left panel of Fig. 5.1, $\mathcal{T}_{\mathcal{RS}}$ is $\mathcal{O}(1)$ at the end of inflation. Therefore it can reduce the value of tensor scalar ratio in contrast to the single 3-form case.

[12] We confront our results with $\chi_i^2 + b_i\chi_i^4$ potential, and one can find make similar predictions with $\chi_i^2 + b_i\chi_i^3$ potential. We do not consider to explore quadratic potential as it is equivalent to inflation with canonical scalar fields (in dual picture).

[13] In the single 3-form case [23, 22] and also in the type I solution of two 3-forms case, this additional slow roll parameter satisfies, $s \equiv \frac{\dot{c}_s}{c_s H} = 0$.

Evidently two 3-forms inflation can be observationally distinguished from single 3-form inflation, due to the possibility of a varying speed of sound (cf. section 3.2.2) and transfer function corrections by the end of inflation. Our method of observational analysis are quite similar to the studies in [43, 41]. In the following we confront our results against Planck+WP+BAO data which provides $\frac{dn_s}{d\ln k} = -0.013 \pm 0.009$ for the running of spectral index, and $\frac{d^2 n_s}{d\ln k^2} = 0.017 \pm 0.009$ for the running of running spectral index, both at 95% CL, which rules out exact scale-invariance at more than 5σ level. Our analysis show that for type II solution, a better fit can be achieved given the current observational bounds (ruling out exact scale-invariance).

In Figs. 5.2 and 5.3, obtained through suitable data manipulating programs [54, 55], we have examined various types of potentials for a reasonable fit to the observational constraints by Planck. In addition, we have also considered the possibility of a higher tensor scalar ratio, since the latest B-mode polarization analysis (BICEP2) discards a tensor scalar ratio value $r = 0$ at 7σ [28]. We found that potentials such as $V_i = V_{i0}\left(\chi_i^2 + b_i\chi_i^4\right)$ allow favorable contrast of two 3-forms inflation scenario against recent observational data. The parameter b_i, in the mentioned potential, is adequately chosen, so that the speed of sound gets bounded by $0.02 \lesssim c_s^2 < 1$, in order to comply with the Planck constraint. We found that type II inflation, obtained through a small asymmetry in the slopes of the potentials (making $V_{10} \neq V_{20}$), is needed to fit the parameters within the bounds of the observational data, especially for the running and running of running spectral indexes. There are two relevant aspects that should be mentioned regarding this comparison; one is related to the property of type II solution for computing the running of the spectral index. This is a consequence of the varying speed of sound, which is natural for this solution. The other aspect is the requirement of the asymmetry between the potentials. This leads to a mild generation of isocurvature perturbations towards the end of inflation, which can accommodate tensor scalar ratio values within the present bounds of Planck or with BICEP2 data as well. We note that solutions with large curved trajectory in field space can lead to values for inflationary parameters beyond the observational bounds. The presence of curvature, in the field space trajectories, implies a peculiar imprint in the primordial bispectrum during multiple field inflation [41]. Therefore, a natural extension of this work is to study the non-Gaussianity for two 3-form inflation [56].

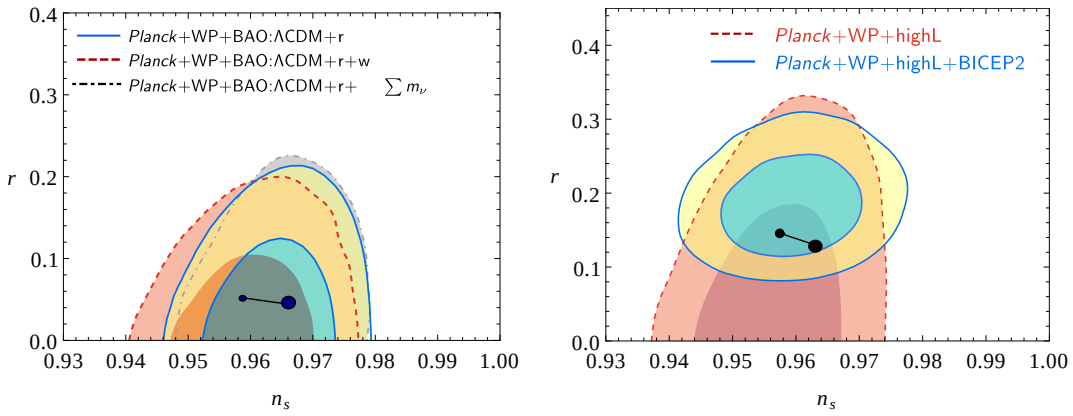


Figure 5.2: Graphical representation of the spectral index versus the tensor to scalar ratio, in the background of Planck+WP+BAO data (left panel), for $N_* = 60$ number of e-folds before the end of inflation (large dot) and $N_* = 50$ (small dot). We have taken $V_1 = V_{10}(x_1^2 + bx_1^4)$ and $V_2 = V_{20}(x_2^2 + bx_2^4)$ where $V_{10} = 1$, $V_{20} = 0.93$, $b = -0.35$ for two 3-form. The right panel corresponds to n_s versus r in the background of Planck+WP+highL+BICEP2 data. We have taken the potentials $V_1 = V_{10}(x_1^2 + b_1x_1^4)$ and $V_2 = V_{20}(x_2^2 + b_2x_2^4)$ where $V_{10} = 1$, $V_{20} = 0.99$, $b_1 = -0.14$, $b_2 = -0.122$. This figure was obtained by taking the initial condition $\theta = \pi/4$.

6 Conclusions, discussion and outlook

Let us summarize our specific results. Inflation driven by a multifield setting, in particular by a couple of 3-form fields, is very much still admissible within current Planck or BICEP2 data. This is the main assertion that this work indicates. Moreover, two 3-form fields with a small asymmetry (in the sense explained in this paper) produces better results (in terms of fitting within current observational data) for concrete cosmological parameters, in contrast to a symmetric configuration or to a single 3-form setting. This is interesting if we take into consideration, the correspondence (on dualization) between 3-form field and non-canonical (kinetical) scalar field dynamics. In fact, a dual description of two 3-

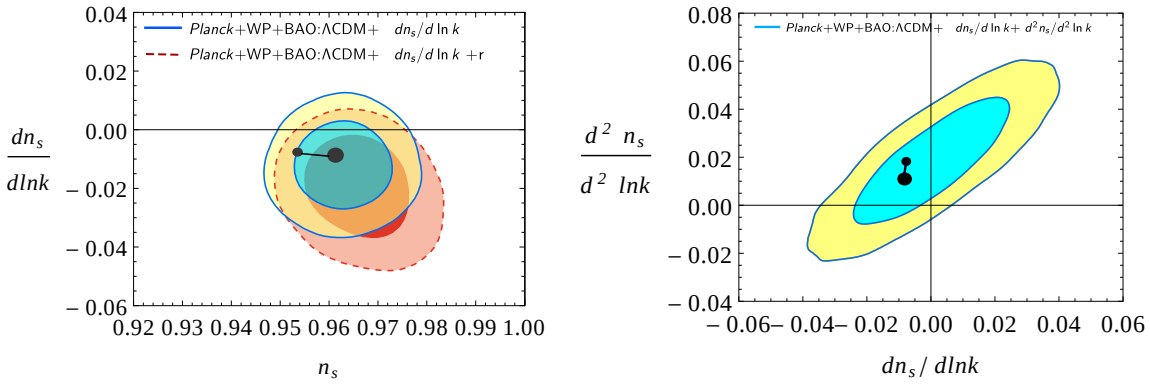


Figure 5.3: Graphical representation of the running of the spectral index versus the spectral index (left panel), and running of the running of the spectral index versus the running of the spectral index (right panel) in the background of Planck+WP+BAO data for $N_* = 60$ number of e-folds before the end of inflation (large dot) and $N_* = 50$ (small dot). We have taken $V_1 = V_{10}(x_1^2 + bx_1^4)$ and $V_2 = V_{20}(x_2^2 + bx_2^4)$ where $V_{10} = 1$, $V_{20} = 0.93$, $b = -0.35$ for two 3-form. This figure was also obtained by taking the initial condition $\theta = \pi/4$.

forms assists to relate to k-inflationary models [9]. First, we have shown that having multiple 3-forms driven inflation brings the inflaton mass to a lower scale, when compared with a single 3-form. We then identified the existence of de Sitter like fixed points, where two 3-forms inflation can mimic single 3-form inflationary scenarios, for a suitable class of potentials. We also did a detailed numerical study of a different type of inflationary dynamics (type II) characterized by the dominance of a non trivial (gravity mediated) coupling, between the two 3-form fields. The type II solution stands physically interesting by its ability to generate substantial isocurvature perturbations at the end of inflation. We have numerically computed the effect of these perturbations via transfer functions. The comparison of selected inflationary parameters against the observational data, in the case where the 3-form fields potential have the form $\chi_i^2 + b_i\chi_i^4$, show that type II solutions, predicting a small variation in the speed of sound, are in excellent agreement with the observational bounds of running spectral indexes.

Subsequent tentative lines of exploration, following the herein paper can be as follows. It would be interesting to explore the generation of isocurvature perturbations and how they impact on the primordial non-Gaussianity and the bispectrum. The gravity mediated coupling through the $\dot{H}$-term in the equations of motion can be explored in the context of reheating phase after inflation or at the late time dark energy scenarios with multiple 3-forms [57, 58].

Acknowledgments

Sravan Kumar is grateful for the support of grant SFRH/BD/51980/2012 from Portuguese Agency Fundação para a Ciência e Tecnologia. This research work was supported by the grants CERN/FP/123615/2011, CERN/FP/123618/2011, PEst-OE/FIS/UI2751/2014 and PEst-OE/MAT/UI0212/2014. This work was also based on observations obtained with Planck (http://www.esa.int/Planck), an ESA science mission with instruments and contributions directly funded by ESA Member States, NASA, and Canada; and BICEP2 2014 (http://bicepkeck.org./). We also thanks the COSMOMC team for the resources and software available at http://cosmologist.info/cosmomc.

A Appendix: Stability of type I fixed points

Let us now discuss the stability of these fixed points for specific choice of potentials. The eigenvalues of $\mathcal{M}_{ij}$ corresponding to the fixed point (x_{1c}, w_{1c}) are $\zeta_1 = -3$, $\zeta_2 = 0$. Since the second eigenvalue is zero, we cannot decide on the stability of this fixed point. The eigenvector for the null eigenvalue is given by

$$v_0 = \begin{pmatrix} \sqrt{2/3} \\ 1 \end{pmatrix}. \tag{A.1}$$

Let us consider the nonlinear order perturbation in the expansion

$$\delta r' = \mu^{(n)}\delta r^n \tag{A.2}$$

where $\delta r = \sqrt{2/3}\delta x_1 + \delta w_1$ is the perturbation along the direction of the eigenvector (A.1). The general solution of Eq. (A.2) at order n is

$$\frac{\delta r^{(-n+1)}}{(-n+1)} = \mu^{(n)} N + \frac{\delta r_0^{(-n+1)}}{(-n+1)} \quad \text{with} \quad \delta r_0 = \delta r \ (N = 0)\,. \tag{A.3}$$

For $n > 1$, an initial negative perturbation $\delta r_0 < 0$ will decay if $\mu^{(n)}$ is positive, with n even, or $\mu^{(n)}$ is negative and n odd. If the initial perturbation is positive, then it will decay for $\mu^{(n)}$ is negative, for all $n > 1$. If we require that $\mu^{(1)} = 1$ in Eq. (A.2), we must have $\delta x_1 = \sqrt{3/2}\delta r/2$ and $\delta w_1 = \delta r/2$. The procedure consists in evaluating

$$\delta r' = \sqrt{2/3}\delta x_1' + \delta w_1' \tag{A.4}$$

and collecting the second order terms of the expansion of eqs. (3.9) and (3.10) when the dynamical system is perturbed around the fixed point

$$\begin{aligned} x_1 &= \sqrt{\frac{2}{3}}\cos\theta + \delta x_1 \\ w_1 &= \cos\theta + \delta w_1 . \end{aligned}$$

As the constraint (3.6) imposes that the dynamical system, near the fixed point, can only be subjected to a small negative perturbation, thus, we will consider an initial negative perturbation $\delta r_0 < 0$. Otherwise, a positive perturbation, that would slightly increase the value of the two fields above the fixed point, would imply that the Friedmann constraint (3.4) would blow up to infinity.

As it is seen from of eqs. (3.9) and (3.10), the presence of the functions λ_1 and λ_2, which, in turn, depend on the potentials and their derivatives, does not allow to study in general the stability of the type I solutions. Therefore, we illustrate this study for some simple and suitable choice of potentials.

A.1 Identical quadratic potentials

Let us consider the simple case when the two fields are under the influence of identical quadratic potentials, i.e., $V(x_1) = x_1^2$ and $V(x_2) = x_2^2$. In this situation, Eqs. (3.10) and (3.12) exhibit type I solutions for any $0 < \theta < \pi/2$. The fixed points for these solutions are constrained by Eq. (3.15). Collecting the second order term in (A.4) we have

$$\mu^{(2)} = -\frac{9}{4}\Big(3\cos\theta + \cos 3\theta\Big), \tag{A.5}$$

which is always negative for $0 < \theta \leq \pi/4$. This means that all fixed points with $0 < \theta < \pi/4$ are unstable. If θ gets larger than $\pi/4$ then the fixed point coordinates $x_{2c} > x_{1c}$ and we can also collect the second order terms in $\delta r' = \sqrt{2/3}\delta x_2' + \delta w_2'$ for a negative perturbation $x_2 = \sqrt{\frac{2}{3}}\sin\theta + \delta x_2$. The coefficient yields

$$\mu^{(2)} = -\frac{9}{4}\Big(3\sin\theta - \sin 3\theta\Big), \tag{A.6}$$

which is always negative for $\pi/4 \leq \theta < \pi/2$. When the angle θ is close to $\pi/2$, then the 3-form field x_1 approaches zero and Eq. (A.5) produces positive values for $\mu^{(2)}$. This means that in the asymmetric situation where $x_1 \approx 0$ and $x_2 \approx \sqrt{2/3}$, the solution $x_1(N)$ converges to zero, however $x_2(N)$ will be unstable. In fact, from Eq. (A.6), the second field will eventually diverge from $\sqrt{2/3}$, when subjected to a small negative perturbation. Furthermore, the decrease in the value of x_2 implies that the variable w_2 will start to fall faster, as Eq. (3.11) suggests. The decrease of x_2 will proceed until it reaches zero. At this point, we can show that both fields will start to oscillate around zero with a damping factor. The discussion for the situation where θ is near zero, is the same, in the sense that the roles of x_1 and x_2, in the previous discussion, are interchanged. In Fig. 3.1 (left panel), the behavior of the two fields, at the end of the inflationary period, when the angle θ is close to $\pi/2$, are shown. Therein, we see that the two fields are going to a damped oscillatory regime, after the divergence of x_2 from its fixed point. The herein analytical description is numerically confirmed.

A.2 Quadratic and quartic potentials

When the two fields are subjected to the potentials $V(x_1) = x_1^2$ and $V(x_2) = x_2^4$, the evolution is generally of the type II. However, Eqs. (3.10) and (3.12) exhibit type I solutions when the condition (3.17) holds, which in this case becomes

$$\left(\frac{1}{\frac{3}{4}(\cot\theta)^2\csc\theta + \sin\theta}\right)^2 + \left(\frac{6\cos\theta}{6 - \cos 2\theta + \cos 4\theta}\right)^2 = 1. \tag{A.7}$$

This last condition is satisfied for $\theta \to \pi/3$, $\theta \to \pi/2$ and at $\theta \to 0$. Collecting the second order term in (A.4) we have

$$\mu^{(2)} = -\frac{3}{5}, \tag{A.8}$$

which is negative. This means that the fixed point with $\theta = \pi/3$ is unstable. At $\theta = 0$,i.e, the scenario with the quadratic term dominance, we must go to third order since, $\mu^{(2)} = 0$. In that case, collecting the third order terms we have $\mu^{(3)} = 0.28$, which means that the fixed point is unstable. At $\theta = \pi/2$, scenario with the quartic term dominance, $\mu^{(2)} = -7.5$, which means that the fixed point is unstable.

References

[1] P.A.R. Ade et al. Planck 2013 results. XXII. Constraints on inflation. 2013.

[2] P.A.R. Ade et al. Planck 2013 results. XVI. Cosmological parameters. 2013.

[3] P.A.R. Ade et al. Planck 2013 results. XVII. Gravitational lensing by large-scale structure. 2013.

[4] C.L. Bennett, D. Larson, J.L. Weiland, N. Jarosik, G. Hinshaw, et al. Nine-Year Wilkinson Microwave Anisotropy Probe (WMAP) Observations: Final Maps and Results. 2012.

[5] David Wands. Multiple field inflation. *Lect.Notes Phys.*, 738:275–304, 2008.

[6] Andrei D. Linde. Hybrid inflation. *Phys.Rev.*, D49:748–754, 1994.

[7] Andrew R. Liddle, Anupam Mazumdar, and Franz E. Schunck. Assisted inflation. *Phys.Rev.*, D58:061301, 1998.

[8] Edmund J. Copeland, Anupam Mazumdar, and N.J. Nunes. Generalized assisted inflation. *Phys. Rev.*, D60:083506, 1999.

[9] Junko Ohashi and Shinji Tsujikawa. Observational constraints on assisted k-inflation. *Phys.Rev.*, D83:103522, 2011.

[10] Frederico Arroja, Shuntaro Mizuno, and Kazuya Koyama. Non-gaussianity from the bispectrum in general multiple field inflation. *JCAP*, 0808:015, 2008.

[11] S. Dimopoulos, S. Kachru, J. McGreevy, and Jay G. Wacker. N-flation. *JCAP*, 0808:003, 2008.

[12] Panagiota Kanti and Keith A. Olive. Assisted chaotic inflation in higher dimensional theories. *Phys.Lett.*, B464:192–198, 1999.

[13] Andrew R. Frey and Anupam Mazumdar. Three form induced potentials, dilaton stabilization, and running moduli. *Phys.Rev.*, D67:046006, 2003.

[14] Steven S. Gubser. Supersymmetry and F theory realization of the deformed conifold with three form flux. 2000.

[15] L.H. Ford. Inflation driven by a vector field. *Phys.Rev.*, D40:967, 1989.

[16] Tomi Koivisto and David F. Mota. Vector Field Models of Inflation and Dark Energy. *JCAP*, 0808:021, 2008.

[17] Alexey Golovnev, Viatcheslav Mukhanov, and Vitaly Vanchurin. Gravitational waves in vector inflation. *JCAP*, 0811:018, 2008.

[18] Cristiano Germani and Alex Kehagias. P-nflation: generating cosmic Inflation with p-forms. *JCAP*, 0903:028, 2009.

[19] S. Koivisto, David F. Mota, and Cyril Pitrou. Inflation from N-Forms and its stability. *JHEP*, 0909:092, 2009.

[20] Tsutomu Kobayashi and Shuichiro Yokoyama. Gravitational waves from p-form inflation. *JCAP*, 0905:004, 2009.

[21] Tomi S. Koivisto and Nelson J. Nunes. Three-form cosmology. *Phys.Lett.*, B685:105–109, 2010.

[22] Tomi S. Koivisto and Nelson J. Nunes. Inflation and dark energy from three-forms. *Phys.Rev.*, D80:103509, 2009.

[23] Antonio De Felice, Khamphee Karwan, and Pitayuth Wongjun. Stability of the 3-form field during inflation. *Phys.Rev.*, D85:123545, 2012.

[24] Antonio De Felice, Khamphee Karwan, and Pitayuth Wongjun. Reheating in 3-form inflation. *Phys.Rev.*, D86:103526, 2012.

[25] David J. Mulryne, Johannes Noller, and Nelson J. Nunes. Three-form inflation and non-Gaussianity. *JCAP*, 1212:016, 2012.

[26] David Langlois and Sebastien Renaux-Petel. Perturbations in generalized multi-field inflation. *JCAP*, 0804:017, 2008.

[27] D.H. Lyth and A.R. Liddle. *The Primordial Density Perturbation: Cosmology, Inflation and the Origin of Structure*. Cambridge University Press, 2009.

[28] P.A.R. Ade et al. BICEP2 I: Detection of B-mode Polarization at Degree Angular Scales. 2014.

[29] A. Ashoorioon and M.M. Sheikh-Jabbari. Gauged M-flation, its UV sensitivity and Spectator Species. *JCAP*, 1106:014, 2011.

[30] A. Ashoorioon, U. Danielsson, and M.M. Sheikh-Jabbari. 1/N Resolution to Inflationary η-Problem. *Phys.Lett.*, B713:353–357, 2012.

[31] H. K. Khalil. *Nonlinear Systems*. Englewood Cliffs. NJ: Prentice Hall, 1996.

[32] Jack Carr. *Applications of Center Manifold Theorem*. Springer-Verlag, 1981.

[33] P. Holmes J. Guckenheimer. *Nonlinear Oscillations, Dynamical Systems and Bifurcation of Vector Fields*. Springer-Verlag, 1983.

[34] Christian G. Böhmer, Nyein Chan, and Ruth Lazkoz. Dynamics of dark energy models and centre manifolds. *Phys.Lett.*, B714:11–17, 2012.

[35] Antonio De Felice, Khamphee Karwan, and Pitayuth Wongjun. Stability of the 3-form field during inflation. *Phys. Rev. D*, 85:123545, Jun 2012.

[36] Jonathan Braden, Lev Kofman, and Neil Barnaby. Reheating the Universe After Multi-Field Inflation. *JCAP*, 1007:016, 2010.

[37] Ian Huston and Adam J. Christopherson. Calculating Non-adiabatic Pressure Perturbations during Multi-field Inflation. *Phys.Rev.*, D85:063507, 2012.

[38] Adam J. Christopherson and Karim A. Malik. The non-adiabatic pressure in general scalar field systems. *Phys.Lett.*, B675:159–163, 2009.

[39] Christopher Gordon, David Wands, Bruce A. Bassett, and Roy Maartens. Adiabatic and entropy perturbations from inflation. *Phys.Rev.*, D63:023506, 2001.

[40] David Langlois, Sebastien Renaux-Petel, and Daniele A. Steer. Multi-field DBI inflation: Introducing bulk forms and revisiting the gravitational wave constraints. *JCAP*, 0904:021, 2009.

[41] David I. Kaiser, Edward A. Mazenc, and Evangelos I. Sfakianakis. Primordial Bispectrum from Multifield Inflation with Nonminimal Couplings. *Phys.Rev.*, D87(6):064004, 2013.

[42] Z. Lalak, D. Langlois, S. Pokorski, and K. Turzynski. Curvature and isocurvature perturbations in two-field inflation. *JCAP*, 0707:014, 2007.

[43] Courtney M. Peterson and Max Tegmark. Testing Two-Field Inflation. *Phys.Rev.*, D83:023522, 2011.

[44] Maciej Konieczka, Raquel H. Ribeiro, and Krzysztof Turzynski. The effects of a fast-turning trajectory in multiple-field inflation. 2014.

[45] David Wands, Nicola Bartolo, Sabino Matarrese, and Antonio Riotto. An Observational test of two-field inflation. *Phys.Rev.*, D66:043520, 2002.

[46] N. Bartolo, S. Matarrese, and A. Riotto. Adiabatic and isocurvature perturbations from inflation: Power spectra and consistency relations. *Phys.Rev.*, D64:123504, 2001.

[47] Filippo Vernizzi and David Wands. Non-gaussianities in two-field inflation. *JCAP*, 0605:019, 2006.

[48] Joseph Elliston, David J. Mulryne, and Reza Tavakol. What Planck does not tell us about inflation. *Phys.Rev.*, D88:063533, 2013.

[49] Ki-Young Choi, Jinn-Ouk Gong, and Donghui Jeong. Evolution of the curvature perturbation during and after multi-field inflation. *JCAP*, 0902:032, 2009.

[50] Justin Khoury and Federico Piazza. Rapidly-Varying Speed of Sound, Scale Invariance and Non-Gaussian Signatures. *JCAP*, 0907:026, 2009.

[51] Minjoon Park and Lorenzo Sorbo. Sudden variations in the speed of sound during inflation: Features in the power spectrum and bispectrum. *Phys. Rev. D*, 85:083520, Apr 2012.

[52] Yi-Fu Cai, James B. Dent, and Damien A. Easson. Warm DBI Inflation. *Phys.Rev.*, D83:101301, 2011.

[53] Anastasios Avgoustidis, Sera Cremonini, Anne-Christine Davis, Raquel H. Ribeiro, Krzysztof Turzynski, et al. The Importance of Slow-roll Corrections During Multi-field Inflation. *JCAP*, 1202:038, 2012.

[54] Antony Lewis and Sarah Bridle. Cosmological parameters from CMB and other data: a Monte-Carlo approach. *Phys. Rev.*, D66:103511, 2002.

[55] Antony Lewis. Efficient sampling of fast and slow cosmological parameters. *Phys. Rev.*, D87:103529, 2013.

[56] Two 3-forms inflation non Gaussianity. *In preparation.*

[57] Tomi S. Koivisto and Nelson J. Nunes. Coupled three-form dark energy. D88:123512, 2013.

[58] T. Ngampitipan and P. Wongjun. Dynamics of three-form dark energy with dark matter couplings. *JCAP*, 1111:036, 2011.